Hierarchical model in multiphase flow

Tohru Okuzono,[1] Hirohisa Shibuya,[2] and Masao Doi[2]
[1]*Institute for Nonlinear Sciences and Applied Mathematics, Hiroshima University, Higashi-Hiroshima 739-8526, Japan*
[2]*Department of Computational Science and Engineering, Nagoya University, Nagoya 464-8603, Japan*
(Received 19 October 1999)

A hierarchical model for two-phase flow is constructed. The model has two layered systems one corresponding to the macroscopic hydrodynamics described by the Navier-Stokes equation and the other to the interfacial dynamics described by the Cahn-Hilliard-type equation. Numerical simulations in some simple cases are carried out to examine the validity of the model. As an application of the model simulations of two colliding droplets under shear flow are presented.

PACS number(s): 83.10.Lk, 68.10.−m, 82.70.−y, 47.11.+j

I. INTRODUCTION

When we intend to perform a numerical simulation of complex flows such as turbulent flows in geophysical systems or microhydrodynamical flows in soft materials, we often encounter the difficulty that the resolution is too low with a macroscopic model or the system size is too small with a microscopic model to obtain significant results. This is due to the fact that a nonlinearity of governing equations causes an interference among degrees of freedom with different scales or the fact that macroscopic processes are inevitably affected by more microscopic processes which are not averaged out. It is worth while studying a numerical method to connect a model with another one, where the scales of the phenomena described by the two models are different. To our knowledge there is no established method for such connection between models. The aim of this paper is to show a prototype of such method for two-phase flow systems.

In two-phase flow systems, interfaces between the two phases play an important role. Let us imagine a coalescence of two droplets. This event occurs in a small scale region which has comparable size to the interface thickness, while it causes a change of global structure of the domains. This means the dynamics of interfaces is crucial for the macroscopic two-phase flows. In a macroscopic hydrodynamical treatment they are formulated as boundary value problems with moving boundaries where the interfaces are regarded as mathematical surfaces or boundaries with an infinitesimal thickness. (For a recent review of the free-surface flow problems, see Ref. [1].) From a numerical view point, it is a heavy task to solve these problems for complex systems. Moreover, the coalescence of domains must be incorporated on some artificial assumptions.

On the other hand, as long as slow dynamics of phase ordering systems [5], there is a mesoscopic model to describe the dynamics of the order parameter field where the interface is expressed as a singular region of the field. Since the order parameter field is smooth even in the interfacial regions, the coalescence of domains are naturally described with no artificial assumptions. However, the size of interfacial region or the interface thickness is very small compared to the typical domain size in the systems which we would like to consider. For some materials, the ratio of the interface thickness to the domain size is 10^{-2}–10^{-4} [2]. To obtain rheological properties of some dispersion system, for example, we must carry out a simulation in a huge system.

In order to overcome these difficulties a certain kind of multiscale modeling should be explored. As a first step, we would like to model a simple but nontrivial system in view of the multiscale modeling. In our model the mesoscopic dynamics is incorporated into the macroscopic hydrodynamical model, and the system is constructed with two layered systems corresponding to the macroscopic and mesoscopic dynamics. Since the mesoscopic dynamics is relevant only near the interface, we can reduce computational tasks by restricting domains of computation within the interfacial regions.

This paper is organized as follows. In the next section we construct a two level model after introducing the macroscopic and mesoscopic models. Next, we carry out numerical simulations in some simple cases and demonstrate their results. We also present some results of the simulation which is performed on droplet systems under shear flows. Finally, we summarize this work.

II. HIERARCHICAL MODELING

A. Macroscopic hydrodynamic equations in a two-phase system

Macroscopic two-phase flows in isothermal systems are usually formulated by the Navier-Stokes equations and boundary conditions at interfaces between the two phases. In this paper we study low Reynolds number fluids so that the convection term can be neglected. For two immiscible fluids A and B, the governing equations with no body forces are

$$\rho_\alpha \frac{\partial \boldsymbol{v}_\alpha}{\partial t} = -\nabla p_\alpha + \eta_\alpha \Delta \boldsymbol{v}_\alpha, \tag{1}$$

$$\nabla \cdot \boldsymbol{v}_\alpha = 0, \tag{2}$$

where $\alpha = A$ or B and ρ_α, $\boldsymbol{v}_\alpha$, p_α, and η_α are the density, the velocity, the pressure, and the shear viscosity of α fluid, respectively. With no mass transfer across the interface, the boundary conditions at the interface are given by

$$\boldsymbol{v}_A - \boldsymbol{v}_B = \boldsymbol{0}, \tag{3}$$

$$(\mathbf{T}_A-\mathbf{T}_B)\cdot\boldsymbol{n}+\sigma\kappa\boldsymbol{n}=\mathbf{0}, \tag{4}$$

where $\boldsymbol{n}$ is the unit normal vector (directed into A) to the interface, $\mathbf{T}_\alpha\equiv -p_\alpha\mathbf{I}+\eta_\alpha(\nabla\boldsymbol{v}_\alpha+\nabla\boldsymbol{v}_\alpha^T)$ is the stress tensor ($\mathbf{I}$ is the unit tensor and $\nabla\boldsymbol{v}_\alpha^T$ is the transpose of the tensor $\nabla\boldsymbol{v}_\alpha$), σ is the surface tension, and κ is the mean curvature of the interface defined as the sum of principal curvatures. Here we have assumed that the surface tension σ is constant.

B. Model in interfacial regions

The above model does not describe a precise dynamics of a system which has diffusive interfaces. In order to describe the proper dynamics of two-phase flow in the interfacial regions, we employ the Cahn-Hilliard-type model under existence of flow field which is called ''model H'' according to the terminology of the critical dynamics [3,4]. This model has been used to describe the dynamics of phase separation [5–8].

We consider a phase-separating binary fluid mixture which is characterized by a scalar order parameter field. The order parameter field corresponds to local concentration difference between the two phases. Let $\psi(\boldsymbol{r},t)$ be the order parameter field at position $\boldsymbol{r}$ and time t, and $\boldsymbol{v}(\boldsymbol{r},t)$ the local velocity field of the fluid. Time evolution of the system is determined by the following set of equations in the absence of thermal fluctuations (hereafter we omit the arguments of the variables unless any confusion arises):

$$\frac{\partial\psi}{\partial t}+(\boldsymbol{v}\cdot\nabla)\psi=L\Delta\mu, \tag{5}$$

$$\rho\frac{\partial\boldsymbol{v}}{\partial t}=-\nabla p+\mu\nabla\psi+\nabla\cdot[\,\eta(\nabla\boldsymbol{v}+\nabla\boldsymbol{v}^T)], \tag{6}$$

$$\nabla\cdot\boldsymbol{v}=0, \tag{7}$$

where L is the kinetic coefficient, ρ the fluid density which is assumed to be constant independent of ψ, p the pressure, and η the shear viscosity.

Equation (5) represents the conservation of ψ with the diffusion flux $-L\nabla\mu$. The chemical potential μ is derived from the free energy functional $F[\psi]$ as $\mu=(\delta/\delta\psi)F[\psi]$. We assume the following Ginzburg-Landau type free energy for $F[\psi]$:

$$F[\psi]=\int d\boldsymbol{r}\left[\frac{K}{2}|\nabla\psi|^2-\frac{\epsilon}{2}\psi^2+\frac{g}{4!}\psi^4\right], \tag{8}$$

where K, ϵ, and g are positive constants.

The surface tension term, the second term on the right hand side of Eq. (6), arises in the Navier-Stokes equation (6) due to inhomogeneity of ψ. The shear viscosity η may depend on ψ. We expand it with respect to ψ up to the first order, that is, $\eta=\eta_0+\eta_1\psi$ with constants η_0 and η_1.

We now put the above equations into dimensionless form. Let l_0 and t_0 be units of space and time, respectively. The velocity and the order parameter are, respectively, scaled by $u_0\equiv l_0/t_0$ and $\psi_0\equiv(6\epsilon/g)^{1/2}$ which is the equilibrium value of the order parameter. We introduce dimensionless parameters $\xi\equiv[K/(\epsilon l_0^2)]^{1/2}$ and $D\equiv L\epsilon/(u_0 l_0)$ which determine the units of space and time, respectively. Note that $l_0=(K/\epsilon)^{1/2}$ and $t_0=K/(L\epsilon^2)$ when $\xi=D=1$, and they give the interface thickness and diffusion time, respectively. Using these scalings, the model equations now become as follows (henceforth we use the same notation for dimensionless variables as for the corresponding variables having physical dimensions):

$$\frac{\partial\psi}{\partial t}+(\boldsymbol{v}\cdot\nabla)\psi=D\Delta\mu, \tag{9}$$

$$\frac{\partial\boldsymbol{v}}{\partial t}=-\nabla p+\Gamma\mu\nabla\psi+PD\nabla[\,\nu(\nabla\boldsymbol{v}+\nabla\boldsymbol{v}^T)], \tag{10}$$

$$\nabla\cdot\boldsymbol{v}=0, \tag{11}$$

with

$$\mu=-\xi^2\Delta\psi-\psi+\psi^3, \tag{12}$$

$$\nu=1+\nu_1\psi, \tag{13}$$

where $\Gamma\equiv\epsilon\psi_0^2/(\rho u_0^2)$, $P\equiv\nu_0/(L\epsilon)$, and ν_0 is the dynamic viscosity when $\psi=0$, that is, $\nu_0=\eta_0/\rho$ and $\nu_1\equiv(\eta_1/\eta_0)\psi_0$. Equations (9)–(13) form a basic model for the dynamics in the interfacial region. The dimensionless parameters Γ, P, and ν_1 characterize physical properties of the system. Note that the surface tension in this system is given by $(2\sqrt{2}/3)(K/\epsilon)^{1/2}\epsilon\psi_0^2$ (see, for example, Ref. [4]), and if we define the dimensionless surface tension σ scaled by $\rho u_0^2 l_0$, it is given by $\sigma=(2\sqrt{2}/3)\xi\Gamma$. It is also noted that the equilibrium solutions with no flow field are given by $\mu=0$ and the interface is defined as a set of points that satisfy $\psi(\boldsymbol{r})=0$.

We now discuss a thin interface limit ($\xi\to 0$) of Eqs. (9)–(11) that should yield the macroscopic equations which correspond to Eqs. (1)–(4). For simplicity, we here consider a Stokesian flow, that is,

$$-\nabla p+\Gamma\mu\nabla\psi+PD\nabla\cdot[\,\nu(\nabla\boldsymbol{v}+\nabla\boldsymbol{v}^T)]=0\ , \tag{14}$$

instead of Eq. (10). We assume that the order parameter field is almost in equilibrium and radii of curvatures of interfaces are always much greater than the interface thickness ξ. In the limit of $\xi\to 0$, ψ can be regarded as a step function, that is, $\psi=+1$ (in A phase) or -1 (in B phase). Equation (14) now becomes, in the bulk regions,

$$-\nabla p+PD(1\pm\nu_1)\Delta\boldsymbol{v}=0, \tag{15}$$

where plus or minus sign in front of ν_1 correspond to the A or B phase, respectively. The boundary condition (4) at the interface can be obtained by integrating Eq. (14) over a small cylindrical region Ω including a part of the interface. The unit normal vector $\boldsymbol{n}$ to the top (or bottom) face of Ω coincides with the normal to the interface. If we introduce a unit vector $\hat{\boldsymbol{n}}(\boldsymbol{r})$ at $\boldsymbol{r}$ around the interface defined as $\hat{\boldsymbol{n}}(\boldsymbol{r})\equiv\nabla\psi/|\nabla\psi|$ which coincides with $\boldsymbol{n}$ at the interface, we have

$$\Delta\psi=(\nabla\cdot\hat{\boldsymbol{n}})|\nabla\psi|+\hat{\boldsymbol{n}}\cdot\nabla\nabla\psi\cdot\hat{\boldsymbol{n}}. \tag{16}$$

When we choose a local coordinate system where one of the coordinates ζ is taken along $\hat{\boldsymbol{n}}$, we obtain from Eqs. (12) and (16), near the interface,

$$\mu = \xi^2 \kappa \frac{\partial \psi}{\partial \zeta} - \xi^2 \frac{\partial^2 \psi}{\partial \zeta^2} - \psi + \psi^3 \tag{17}$$

$$\simeq \xi^2 \kappa \frac{d\psi_e}{d\zeta}, \tag{18}$$

where $\kappa = -\boldsymbol{\nabla} \cdot \hat{\boldsymbol{n}}$ is the sum of principal curvatures of the interface and $\psi_e \equiv \tanh(\zeta/\sqrt{2}\xi)$ is the equilibrium profile of ψ ($\zeta = 0$ at the interface). Using Eq. (18), the integral of the second term of Eq. (14) is expressed as

$$\int_\Omega d\boldsymbol{r} \Gamma \mu \boldsymbol{\nabla} \psi \simeq \int_{-\varepsilon}^{\varepsilon} d\zeta \Gamma \xi^2 \kappa \left(\frac{d\psi_e}{d\zeta} \right)^2 \boldsymbol{n} S, \tag{19}$$

where ε and S are a half of the height and area of the top (or bottom) surface of the cylinder region, respectively ($\varepsilon, S \ll 1$). If we rescale the length by ξ, and $\xi \to 0$, then we have

$$\int_{-\varepsilon}^{\varepsilon} d\zeta \Gamma \xi^2 \kappa \left(\frac{d\psi_e}{d\zeta} \right)^2 = \int_{-\infty}^{\infty} d\tilde{\zeta} \Gamma \tilde{\kappa} \left(\frac{d\psi_e}{d\tilde{\zeta}} \right)^2 = \frac{2\sqrt{2}}{3} \Gamma \tilde{\kappa} = \sigma \kappa, \tag{20}$$

where $\tilde{\zeta} \equiv \zeta/\xi$, $\tilde{\kappa} \equiv \xi \kappa$. Thus we obtain the dimensionless version of Eq. (4) as a boundary condition for Eq. (15). Here we have required that the velocity field is continuous at the interface (also see the Appendix).

C. Two-level model

The model described in the previous section should yield the macroscopic equations in the thin interface limit $\xi \to 0$. However, here we would like to model the macroscopic two-phase flow, keeping ξ finite. Since the order parameter ψ varies in localized regions with scale ξ, while the velocity field $\boldsymbol{v}$ slowly varies, we split the system (9)–(13) into two layered systems corresponding to the macroscopic and mesoscopic systems.

In order to do this, we define a coarse-grained field $\langle u(\boldsymbol{r}) \rangle_h$ for a field $u(\boldsymbol{r})$ at level h as

$$\langle u(\boldsymbol{r}) \rangle_h = \int d\boldsymbol{r}' G_h(\boldsymbol{r} - \boldsymbol{r}') u(\boldsymbol{r}'), \tag{21}$$

where $G_h(\boldsymbol{r} - \boldsymbol{r}')$ is a weight function having the following properties:

$$\int d\boldsymbol{r}' G_h(\boldsymbol{r} - \boldsymbol{r}') = 1, \quad \lim_{h \to 0} G_h(\boldsymbol{r} - \boldsymbol{r}') = \delta(\boldsymbol{r} - \boldsymbol{r}'). \tag{22}$$

The level h represents a degree of coarsening. A typical example of $G_h(\boldsymbol{r} - \boldsymbol{r}')$ is the Gauss function

$$G_h(\boldsymbol{r} - \boldsymbol{r}') = (2\pi h^2)^{-d/2} \exp\left(-\frac{|\boldsymbol{r} - \boldsymbol{r}'|^2}{2h^2} \right), \tag{23}$$

in d-dimensional space. Another example is

$$G_h(\boldsymbol{r} - \boldsymbol{r}') = \begin{cases} V_h^{-1} & |x_i - x_i'| \leqslant h \quad (i = 1, \ldots, d) \\ 0 & \text{otherwise} \end{cases} \tag{24}$$

where x_i (x_i') is the ith component of $\boldsymbol{r}$ ($\boldsymbol{r}'$) and $V_h \equiv (2h)^d$.

Now we consider two layered systems. One is an original system and the other is a coarse-grained system. Symbolically, a coarse-grained field $\langle u \rangle$ for a field u in the original system is expressed as $\langle u \rangle = \mathcal{G} u$ with a linear operator $\mathcal{G}$. Here we have omitted the suffix h to $\langle \cdots \rangle$. Since the operator $\mathcal{G}$ commute with differential operators, interactions between the two systems arise from the nonlinear terms in Eqs. (9)–(13). If these terms are decoupled except for the surface tension term in Eq. (10), our model can be described as follows. The velocity field $\langle \boldsymbol{v} \rangle$ in the coarse-grained system is determined (for given ψ) by

$$\frac{\partial \langle \boldsymbol{v} \rangle}{\partial t} = -\boldsymbol{\nabla} \langle p \rangle + PD \boldsymbol{\nabla} [\, \nu(\langle \psi \rangle)(\boldsymbol{\nabla} \langle \boldsymbol{v} \rangle + \boldsymbol{\nabla} \langle \boldsymbol{v} \rangle^T)] + \boldsymbol{F}, \tag{25}$$

$$\boldsymbol{\nabla} \cdot \langle \boldsymbol{v} \rangle = 0, \tag{26}$$

where $\boldsymbol{F}$ is the force due to inhomogeneity of ψ which should be calculated from the original system as

$$\boldsymbol{F} = \Gamma \langle \mu \boldsymbol{\nabla} \psi \rangle. \tag{27}$$

In the original system the following equation of ψ is solved for given $\langle \boldsymbol{v} \rangle$, after a prolongation of $\langle \boldsymbol{v} \rangle$ from the coarse-grained system,

$$\frac{\partial \psi}{\partial t} + \langle \boldsymbol{v} \rangle \cdot \boldsymbol{\nabla} \psi = D \Delta \mu, \tag{28}$$

where μ is given by Eq. (12).

When the system contains well defined domains, that is, the order parameter ψ is almost in equilibrium, we can define the interfacial region $\mathcal{I}$ as the region in which the condition $|\boldsymbol{\nabla} \psi| > \delta$ for $\delta > 0$ (δ is a constant parameter) and $\mathcal{D}$ to refer to the other region which consists of N connected regions $\mathcal{D}_i$ ($i = 1,2, \ldots, N$), namely, $\mathcal{D} = \cup_{i=1}^N \mathcal{D}_i$ (see Fig. 1). In this situation we may reduce the number of degrees of freedom of the model provided that ψ is almost in equilibrium in $\mathcal{D}$. Equation (28) is solved only in the interfacial region $\mathcal{I}$ with boundary conditions

$$\psi = \overline{\psi}_i, \quad \mu = \overline{\mu}_i \quad \text{on} \quad \partial \mathcal{D}_i \quad (i = 1,2, \ldots, N), \tag{29}$$

where $\partial \mathcal{D}_i$ denotes the boundary of domain $\mathcal{D}_i$, $\overline{\psi}_i$, and $\overline{\mu}_i$ are the boundary values for ψ and μ, respectively. If we assume that ψ rapidly relaxes in $\mathcal{D}_i$, $\overline{\psi}_i$ might be constant and $\overline{\mu}_i = -\overline{\psi}_i + \overline{\psi}_i^3$. Introducing variables $Q_i \equiv \int_{D_i} d\boldsymbol{r} \psi$ ($i = 1, \ldots, N$), $\overline{\psi}_i$ is given by

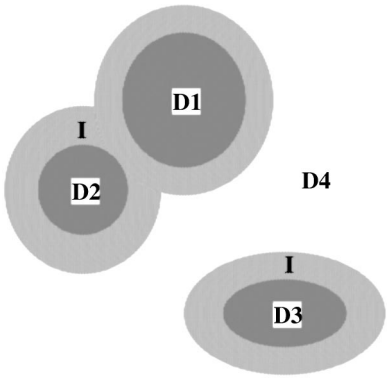

FIG. 1. A schematic picture of domains. The gray regions belong to the interfacial region $\mathcal{I}$ and other regions belong to $\mathcal{D}$.

$$\overline{\psi}_i = Q_i \Big/ \int_{\mathcal{D}_i} d\boldsymbol{r}. \tag{30}$$

The conservation of ψ [Eq. (28)] implies

$$\frac{d}{dt} Q_i = -\int_{\partial \mathcal{D}_i} da\, \boldsymbol{n}_i [\overline{\psi}_i \langle \boldsymbol{v} \rangle + \boldsymbol{\nabla} \mu], \tag{31}$$

where the integral is taken over $\partial \mathcal{D}_i$ (da is a surface element) and $\boldsymbol{n}_i$ is unit normal vector to $\partial \mathcal{D}_i$ (directed outside $\mathcal{D}_i$). Equations (25)–(31) form another version of our model.

III. SIMULATION AND RESULTS

A. Numerical method

In the previous section, two models are constructed. One consists of Eqs. (25)–(28). $\langle \boldsymbol{v} \rangle$ and ψ are solved in the whole regions of the coarse-grained and the original systems, respectively. We refer to this model as model I. The other consists of Eqs. (25)–(31) where ψ is solved only in the interfacial region of the original system, while $\langle \boldsymbol{v} \rangle$ is solved in the whole region of the coarse-grained system. We refer to this model as model II.

We carry out numerical simulations in two-dimensional systems for the model I and a simplified version of model II (see below). For each model (I or II) Eqs. (25)–(28) are numerically solved using the finite difference method on two square lattices L_0 and L_1 corresponding to the coarse-grained and the original systems, respectively. The lattice L_l ($l=0$ or 1) has $M_l \times N_l$ lattice points and mesh size Δ_l. We choose $\Delta_0 = 2\Delta_1$ ($M_0 = M_1/2$, $N_0 = N_1/2$) and a lattice point (i_0, j_0) on L_0 to share the same place as $(2i_1, 2j_1)$ on $L_1 (0 \leq i_0 < M_0,\ 0 \leq j_0 < N_0,\ 0 \leq i_1 < M_1,\ 0 \leq j_1 < N_1)$. The size of a time step Δt_0 in coarse-grained system should be different from that in original system Δt_1. We set $\Delta t_0 = 4\Delta t_1$. Because of numerical convenience, we adopt Eq. (24) as the smoothing function with $h = \Delta_1$. When we need values of $\langle \boldsymbol{v} \rangle$ on L_1 in calculating Eq. (28), we get the values by the bilinear interpolation from $\langle \boldsymbol{v} \rangle$ on L_0. Although ψ is not strictly conserved by this interpolation, the total amount of ψ keeps its initial value within 0.2% error through the simulation shown in the next section.

In the actual simulation shown below we apply a simplification that the boundary values $\overline{\psi}_i$ is always the equilibrium values, that is, $\overline{\psi}_i = \pm 1$ and $\boldsymbol{n}_i \cdot \boldsymbol{\nabla} \mu = 0$ on $\partial \mathcal{D}_i$ so that $dQ_i/dt = 0$. We refer to this model as model II′.

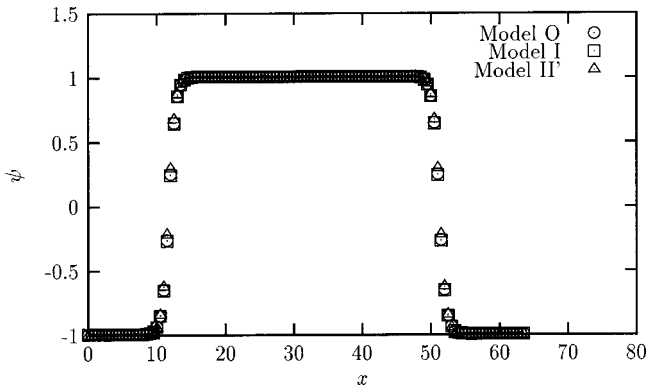

FIG. 2. The profiles of ψ along the line across the center of domain at $t=100$. Results of models O, I, and II′ are shown by circles, squares, and triangles, respectively.

B. Results for some simple systems

The simulations of both models (I and II′) are carried out with the following parameters: $D=1$, $\xi^2 = 0.5$, $\Gamma = P = 1.0$, $\nu_1 = 0.5$, $M_0 = N_0 = 64$, $\Delta_0 = 1.0$, and $\Delta t_0 = 0.01$. For the simulation of model II′ we set $\delta^2 = 0.01$. To compare their results we also perform another simulation of the precise model (9)–(13) on L_1 which we refer to as model O. We impose the periodic boundary conditions on these systems.

We create a disklike domain with radius $R=20$ as an initial condition ($\psi = 1$ or -1 inside or outside of the domain, respectively, and $\boldsymbol{v} = 0$ at every point), and calculate the time evolution of the system for sufficiently long time to get a relaxed system. Figures 2 and 3 shows the profiles of ψ and $\langle p \rangle$, respectively, along the line across the center of the domain for the three models at $t=100$. We can see that the model I is a good approximation of the model O. However, the model II′ slightly underestimates the pressure difference between the inside and outside of domain. This may be because of an underestimation of the surface tension due to the finite cutoff δ for $|\boldsymbol{\nabla} \psi|$. Remember that the surface tension σ for this system is given by $\Gamma \xi^2 \int_{-\infty}^{\infty} (d\psi/d\zeta)^2 d\zeta$, where ζ is a coordinate along the normal to the interface.

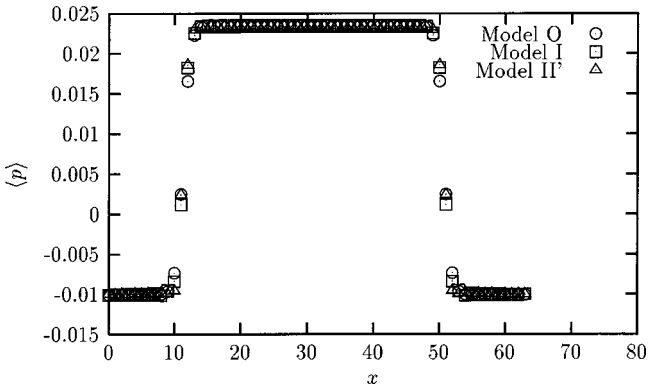

FIG. 3. The profiles of $\langle p \rangle$ along the line across the center of domain at $t=100$. Results of models O, I, and II′ are shown by circles, squares, and triangles, respectively.

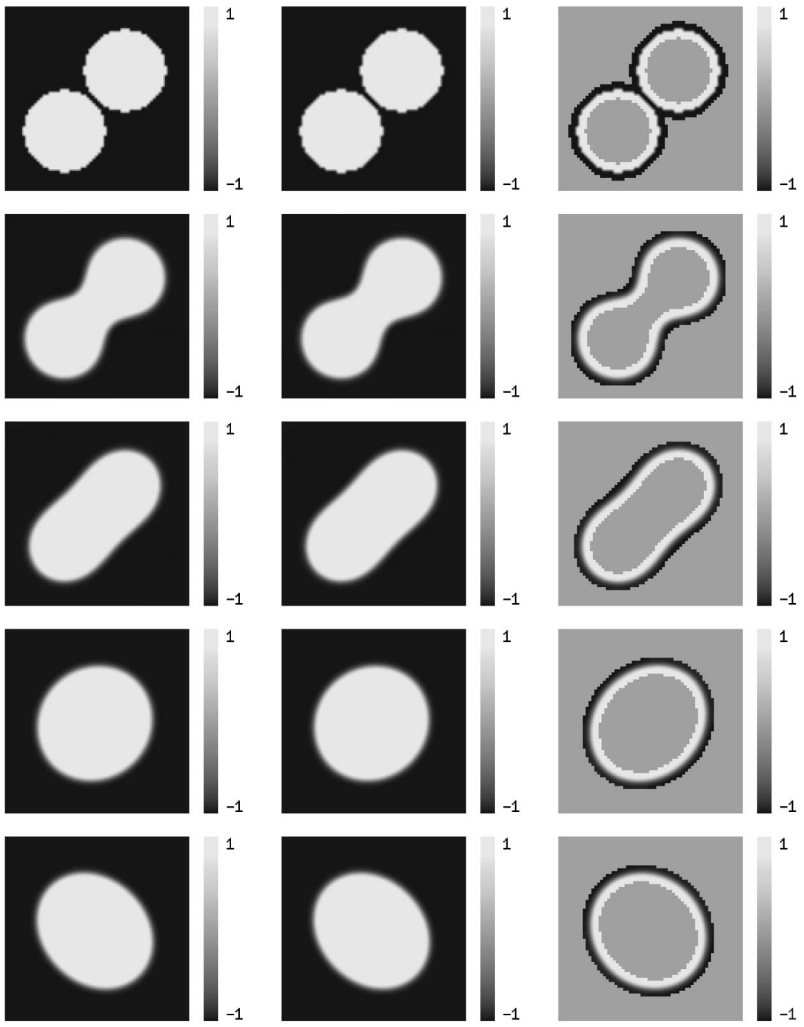

FIG. 4. Snapshots of ψ shown by gray scale. Light (dark) gray indicates large (small) ψ. The figures in the left, middle, and right columns correspond to models O, I, and II′. The time t for the figures from the top to bottom are 0, 50, 100, 200, and 300, respectively. For model II′ ψ is shown only in the interfacial region $\mathcal{I}$.

Next, we investigate a coalescence process of two disklike domains. As an initial condition we put two disklike domains with the same radius $R=\sqrt{200}$ at close positions to each other and set $\boldsymbol{v}=0$ at every point. In Fig. 4 we show the snapshots of ψ for the three models at several times. The figures in the left, middle, and right columns in Fig. 4 correspond to the model O, I, and II′. The time t denoted by the the figures are 0, 50, 100, 200, and 300, respectively, from the top to bottom. In the figures for model II′, ψ is shown only in the interfacial region $\mathcal{I}$. The result of model I shows a good agreement with that of model O. The time evolution of the system for model II′ is slightly slowed down. This is due to the same reason as mentioned above. However, the computation time is greatly reduced for model II′. The real computation times for the simulations of model I and II′ are about 1/6 and 1/10 of the time for model O, respectively.

C. Droplet systems under shear flow

The hydrodynamic study of the deformation, breakup, and coalescence of fluid domains has a long history and extensive studies have been made [1,9–14]. The mesoscopic dynamics of phase separation processes under external flows has also been studied in the last decade [15–17]. As an application of our model, we demonstrate the simulation of droplet systems under shear flows.

We carry out the simulation using model II′ with the parameters: $D=1$, $\xi^2=0.5$, and $\Gamma=1$. These parameters are fixed in the following simulations. To impose the shear we use the sheared periodic boundary condition which requires that $\psi(\boldsymbol{r},t)$ is the periodic function as $\psi(\boldsymbol{r}+\boldsymbol{R}_{mn}(t),t)=\psi(\boldsymbol{r},t)$ and $\boldsymbol{v}(\boldsymbol{r},t)$ satisfies $\boldsymbol{v}(\boldsymbol{r}+\boldsymbol{R}_{mn}(t),t)=\boldsymbol{v}(\boldsymbol{r},t)+\boldsymbol{V}_{mn}$, where $\boldsymbol{R}_{mn}(t)\equiv(mL_x+\dot{\gamma}tnL_y,nL_y)$, $\boldsymbol{V}_{mn}\equiv(\dot{\gamma}nL_y,0)$ with integers m,n; $L_x\equiv\Delta_0 M_0$ and $L_y\equiv\Delta_0 N_0$ are the sizes of simulation box in x and y directions, respectively; $\dot{\gamma}$ is the shear rate.

First, we study a single droplet system under simple shear flows. The numerical parameters are set as $M_0=120$, $N_0=60$, $\Delta_0=1.0$, $\Delta t_0=0.01$, $\delta^2=0.01$. As an initial condition we put a disklike domain (droplet) with radius $R=8$ at the center of the simulation box ($\psi=1$ in the domain and $\psi=-1$ otherwise) and $\boldsymbol{v}(\boldsymbol{r})=(\dot{\gamma}y,0)$. We carry out the simulation with the parameters $P=1$, $\nu_1=0$, and $\dot{\gamma}=-0.05$ and observe morphological change of the domain. In the early time region, the domain is gradually deformed and then reaches a steady state. Figure 5(a) shows a snapshot of ψ in the steady state at $t=240$. We do not observe any breakup of the domain at these parameter values. However, with increasing P we observe breakups of the domains. In Fig. 5(b) we show a snapshot of domains after breakups at $t=240$

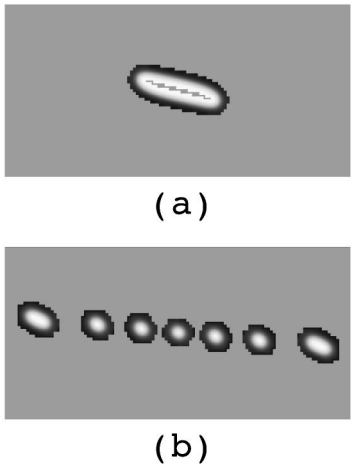

FIG. 5. Snapshots of the single droplet system under the shear flow with $\dot{\gamma}=-0.05$ at $t=240$. ψ are shown by the gray scale in the same manner as before. (a) The droplet is stable and keeps its deformed shape for small P ($P=1,\nu_1=0$). (b) The droplet breaks up for large P ($P=5,\nu_1=0$).

($P=5$, $\nu_1=0$, $\dot{\gamma}=-0.05$). We also perform the simulations varying ν_1. The results are shown in Fig. 6. From these results, it appears that the critical value of P to breakup increases as ν_1 increases when $P>1$. On the other hand, for $P\leqslant 1$ breakup of the domain is not observed.

Next we study a system in which two droplets collide with each other under shear flow. We take $M_0=80$, $N_0=60$ and other parameters are set to the same as before. Initially we put two disklike domains which are sufficiently separated in the system. These droplets are located at $(-15,-7.5)$ and $(15,7.5)$ and have the same radius $R=8$. (Here we have set the origin of coordinate at the center of the simulation box.) By imposing the shear flow, these droplets collide with each other. The simulations are performed for various P and ν_1 to investigate whether the two droplets coalesce or not. The results for $\dot{\gamma}=-0.01$ are summarized in Fig. 7. For small $P(\leqslant 1)$ the two droplets always coalesce irrespectively of ν_1. For $P>1$ they do not coalesce except for the two cases ($P=10$, $\nu_1=-0.6$ and $P=10$, $\nu_1=-0.9$), and their shape are more elongated as ν_1 decreases. These imply that the coalescence of domains is primarily controlled by the parameter P rather than ν_1. However, the coalescence also depends on the viscosity ratio as it is demonstrated by the two exceptional cases of $P=10$, $\nu_1=-0.6$ and $P=10$, $\nu_1=-0.9$. In this case, the droplets coalesce since they are extremely elongated and in contact for a long time which allows enough mass transports between the droplets by diffusion. Figure 8 shows the results for $\dot{\gamma}=-0.05$. At this shear rate no coalescence occurs for $0.5\leqslant P\leqslant 10$ and $-0.9\leqslant\nu_1\leqslant 0.9$ except for the parameters indicated by half-filled circles in Fig. 8 where after the droplets coalesce once, the merged domain separates and become two

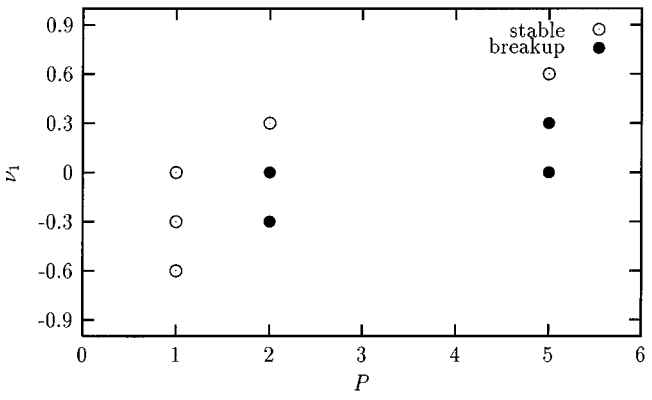

FIG. 6. P-ν_1 dependency of the morphology of a single droplet under the shear flow with $\dot{\gamma}=-0.05$. The empty circles designate the parameters where the droplet is stable. The filled circles designate the parameters where the droplet breaks up.

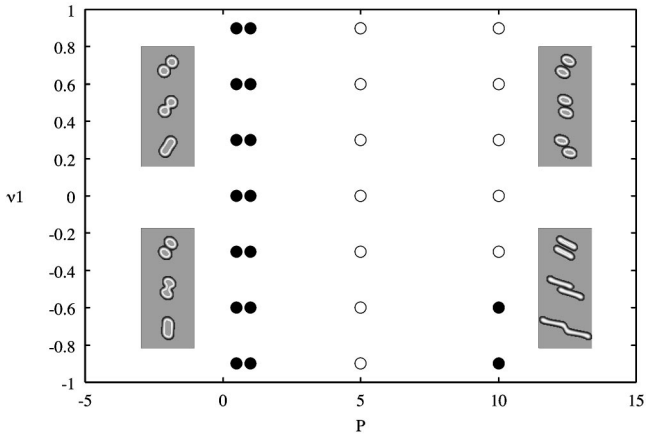

FIG. 7. Diagram that shows morphology of droplets after a collision under the shear flow with $\dot{\gamma}=-0.01$. The droplets coalesce for $P\leqslant 1$ (filled circles), otherwise they do not (empty circles). The inserted images show typical time sequences (from top to bottom) of collisions of droplets. These images are obtained for $P=0.5,\nu_1=0.9$ (upper left), $P=0.5,\nu_1=-0.9$ (lower left), $P=10,\nu_1=0.6$ (upper right), and $P=10,\nu_1=-0.6$ (lower right).

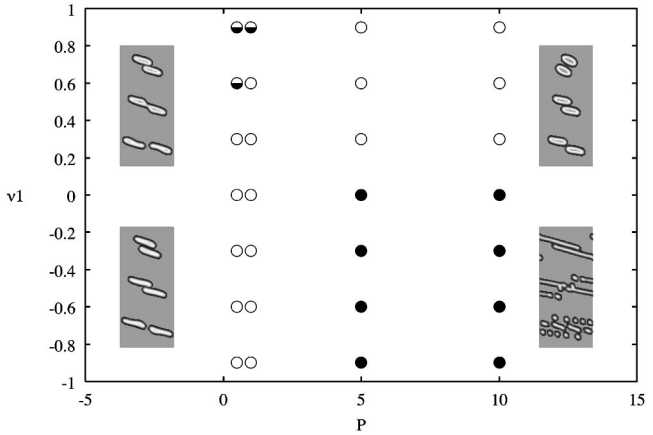

FIG. 8. Diagram that shows morphology of droplets after a collision under the shear flow with $\dot{\gamma}=-0.05$. The droplets separate after a coalescence for small P and large ν_1 (half-filled circles). For large P and small ν_1 they break up (filled circles) and otherwise they do not coalesce (empty circles). The inserted images show typical time sequences (from top to bottom) of collisions of droplets. These images are obtained for $P=0.5,\nu_1=0.6$ (upper left), $P=5.0,\nu_1=0.6$ (upper right), $P=0.5,\nu_1=-0.3$ (lower left), and $P=5.0,\nu_1=-0.9$ (lower right).

droplets again. For $P>1$ and $\nu_1 \leqslant 0$ the droplets break up, which is consistent with the results of the simulation for a single droplet. Although processes of coalescence and breakup of droplets in general situations are rather complicated, our simulations imply that the diffusivity of ψ controlled by P has a primary importance to coalescence or breakup of domains and ν_1 affects deformation or shape of domains for fixed $\dot{\gamma}$, R, and σ.

IV. SUMMARY

We have constructed a model for two-phase flows which is incorporated with the mesoscopic dynamics of interfaces. Our model has two layered systems corresponding to the macroscopic and mesoscopic dynamics, which provides a feasible method to connect the phenomena of different scales.

We have carried out the simulations of the two versions of our model (model I and II′) for the simple initial conditions in two-dimensional systems. The results have been compared to those for the precise model (model O). The results of model I is in good agreement with those of model O. We have, however, observed that for model II′ the surface tension is slightly underestimated and hence the time evolution is slightly slowed down. This is due to the finite cutoff for $|\nabla\psi|$. However, model II′ works most efficiently among the three. We have also demonstrated the simulation of droplet systems under shear flow and shown that the mesoscopic dynamics is important in the process of coalescence or breakup of droplets.

In this study, we have shown a model for rather simple binary fluids as a prototypical example of multiscale modeling. However, our model may be applicable to more complicated system such as two-phase fluids with surfactants or polymers (ternary fluid mixtures) whose dynamical behavior is a critical subject to study. Such an extension of our model is a future problem.

ACKNOWLEDGMENTS

One of the authors (T.O.) would like to thank Professor T. Ohta and Dr. T. Taniguchi for helpful discussions. This research was supported by a grant from the JSPS Research for the Future Program, Computational Science and Engineering.

APPENDIX

In this Appendix we show that the macroscopic velocity field in our model is continuous at the interface in the thin interface limit in a particular case. Consider a flat interface located at $z=0$, that is, $\psi(\boldsymbol{r})=\psi_e(z)=\tanh(z/\sqrt{2}\xi)$ and a shear flow parallel to the interface so that the velocity field has only x component which depends on z, that is, $\boldsymbol{v}(\boldsymbol{r})=(v_x(z),0,0)$. In this case ψ is not dependent on time and the Stokes equation (14) is simplified as

$$\frac{d}{dz}\left[(1+\nu_1\psi_e)\frac{d}{dz}v_x(z)\right]=0. \tag{A1}$$

The solution of this equation is

$$v_x(z)=\sqrt{2}\xi\dot{\gamma}_0\ln\{[1-\psi_e(z)]^{\alpha}[1+\psi_e(z)]^{\beta}[1+\nu_1\psi_e(z)]^{\gamma}\}+u_0, \tag{A2}$$

with

$$\alpha\equiv-\frac{1}{2(1+\nu_1)},\quad \beta\equiv\frac{1}{2(1-\nu_1)},\quad \gamma\equiv-\frac{\nu_1}{1-\nu_1^2}, \tag{A3}$$

where $\dot{\gamma}_0\equiv dv_x(0)/dz$ and $u_0\equiv v_x(0)$. Asymptotic forms $v_x^{\pm}(z)$ of $v_x(z)$ as $z\to\pm\infty$ are given by

$$v_x^{\pm}(z)=\frac{\dot{\gamma}_0}{1\pm\nu_1}z+\frac{\sqrt{2}\xi\dot{\gamma}_0\nu_1}{1-\nu_1^2}\ln\frac{2}{1\pm\nu_1}+u_0. \tag{A4}$$

These may give the macroscopic flow in the bulk phase. If we extrapolate $v_x^{\pm}(z)$ into the interface region, we find that these asymptotic velocities are continuous at $z=z_0[v_x^{+}(z_0)=v_x^{-}(z_0)]$ with

$$z_0=-\frac{\sqrt{2}\xi}{2}\ln\frac{1+\nu_1}{1-\nu_1} \tag{A5}$$

which does not depend on $\dot{\gamma}_0$ and u_0. This means the continuation point ($z=z_0$) of the macroscopic velocities always deviates from the interface ($z=0$) when $\nu_1\neq 0$. However, this deviation vanishes as $\xi\to 0$ and the macroscopic velocities are continuous at the interface in this limit.

[1] J. Eggers, Rev. Mod. Phys. **69**, 865 (1997).
[2] H. Tanaka (private communication).
[3] P.C. Hohenberg and B.I. Halperin, Rev. Mod. Phys. **49**, 435 (1977).
[4] P.M. Chaikin and T.C. Lubensky, *Principles of Condensed Matter Physics* (Cambridge University Press, Cambridge, England, 1995).
[5] J.D. Gunton, M. San Miguel, and P.S. Sahni, in *Phase Transitions and Critical Phenomena*, edited by C. Domb and J. L. Lebowitz (Academic Press, New York, 1983), Vol. 8.
[6] K. Kawasaki and T. Ohta, Physica A **118**, 175 (1983).
[7] T. Koga and K. Kawasaki, Physica A **196**, 389 (1993).
[8] A. Shinozaki and Y. Oono, Phys. Rev. E **48**, 2622 (1993).
[9] G.I. Taylor, Proc. R. Soc. London, Ser. A **138**, 41 (1932).
[10] G.I. Taylor, Proc. R. Soc. London, Ser. A **146**, 501 (1934).
[11] J.M. Rallison and A. Acrivos, J. Fluid Mech. **89**, 191 (1978).
[12] J.M. Rallison, J. Fluid Mech. **109**, 465 (1981).
[13] H.A. Stone, Annu. Rev. Fluid Mech. **26**, 65 (1994).
[14] X.-F. Yuan and M. Doi, Colloids Surf., A **144**, 305 (1998).
[15] T. Ohta, H. Nozaki, and M. Doi, Phys. Lett. A **145**, 304 (1990).
[16] T. Ohta, H. Nozaki, and M. Doi, J. Chem. Phys. **93**, 2664 (1990).
[17] T. Okuzono, Phys. Rev. E **56**, 4416 (1997).